12-25-2005

Properties of Stars in the Subaru Deep Field

Michael Richmond
Rochester Institute of Technology

Recommended Citation
Michael Richmond; Properties of Stars in the Subaru Deep Field, Publications of the Astronomical Society of Japan, Volume 57, Issue 6, 25 December 2005, Pages 969–976, https://doi.org/10.1093/pasj/57.6.969

Properties of Stars in the Subaru Deep Field

Michael Richmond
Physics Department, Rochester Institute of Technology, Rochester, NY 14623
mwrsps@rit.edu

(Received ; accepted)

Abstract

We investigate the properties of objects in the Subaru Deep Field (SDF), using public catalogs constructed from images in several optical passbands. Using a small subset of objects most likely to be stars, we construct a stellar locus in three-dimensional color space. We then compare the position of all objects relative to this locus to create larger samples of stars in the SDF with rough spectral types. The number counts of stars defined in this way are consistent with those of current models of the Galaxy.

Key words: stars: statistics – methods: data analysis

1. Introduction

During the spring seasons of 2002 and 2003, the Subaru telescope and Suprime-Cam mosaic camera acquired very deep images in several passbands of a region of the sky near the North Galactic Pole (Kashikawa et al. 2004). This Subaru Deep Field (SDF) combines a relatively wide area (roughly one third of a square degree) and very deep detection limit (down to magnitude 28 in B), yielding hundreds of thousands of sources with well measured properties. The SDF project team has released to the astronomical community the full imaging dataset as well as a rich set of catalogs, making the SDF a resource which is sure to be used by many groups working in different areas over the next decade.

The primary goals of the SDF project depend on extragalactic sources: using a combination of broadband and narrowband measurements, it is possible to identify objects at redshifts of $z \simeq 4-7$; one can also probe the luminosity function of nearby galaxies to very low levels. In these studies, foreground stars in the Milky Way are annoying contaminants which must be discarded in order to count galaxies properly. We realized, however, that one can also use the SDF catalogs to study the properties of stars themselves. There are very few regions of the sky which have been surveyed as deeply as the SDF, and none at such a high galactic latitude: the Hubble Deep Field North (Williams et al. 1996), for example, is at $b = 54$ degrees, close to an ecliptic pole, as are most other regions studied by satellite-borne instruments. The SDF, at

$l = 37$ and $b = 83$ degrees, provides valuable information on the stellar content of our galaxy in a relatively unexplored direction.

The aim of this paper is twofold: first, to describe in some detail how one can use colors to isolate stars from galaxies in deep imaging surveys; second, to make available to the community the result of our methods applied to sources in the SDF, so that others may easily select new subsets of stellar (or non-stellar) sources. In Section 2, we will describe how one use the colors of stars – as well as their shapes – to distinguish them from galaxies. Stars follow a distinctive path in multidimensional color space, and in Section 3, we demonstrate that their position along this path is a function of spectral type. We then use this stellar locus to assign several new quantities to all objects in one of the SDF catalogs. We show in detail how one can use these new derived quantities to select objects more or less likely to be stars in Section 4. In Section 5, we mention the limitations of our method, which cannot be applied to the full depth of the SDF images. Within its limits, we show that our sample of stars in the SDF is consistent with a model of the Milky Way's stellar component.

2. Defining the Stellar Locus

Kashikawa et al. 2004 describe the acquisition of the images which make up the SDF, the processing of the images, and the creation of a set of catalogs of objects detected in each passband. They placed the processed images and catalogs of objects measured in the field into a public archive, the SDF Data Release. Our analysis is based on these data; in particular, we chose to focus on objects matched to detections in the R_c passband, since it lies in the middle of the spectral range covered by the Suprime-Cam optical filters and since the R_c images are among the deepest in the group. The SDF catalogs matched to the R_c passband contain over $209,000$ objects, the majority of which are distant galaxies. In order to study the properties of the stars which are scattered among these galaxies, one needs a reliable way to distinguish the stars from other objects. Our method requires knowing precisely the region in color-color space occupied by stars, so the first step is to define this stellar locus.

We begin by selecting a "clean" subset of stars from this very large catalog. We tried using the `class_star` values included in Public Data Release. The SExtractor program (Bertin & Arnouts 1996) produces this number, which describes the degree to which an object resembles the PSF; its value ranges from 0.0 (for very extended objects) to 1.0 (for perfect point sources). After examining a number of sources near the center of the SDF carefully, we found that using a simple limit on this `class_star` parameter did a very good, but not perfect, job of identifying stars. Even if one placed a very narrow limit on the range of acceptable values – for example, $0.95 <$ `class_star` < 1.0 – a small number of galaxies would still contaminate the sample of stars.

Therefore, we searched for an additional piece of morphological information to improve the star/galaxy separation. Kashikawa et al. 2004 suggest a combination of magnitude and Full-

Width at Half-Maximum (FWHM). When we used this criterion, we found that a substantial number of galaxies were still mixed with the stars. After some experimentation, we found another parameter which may do a slightly better job of identifying stars: the difference of magnitudes measured through two different circular apertures. Using the catalog fields m_2, the magnitude through an aperture of radius 2 arcseconds, and m_3, the magnitude through an aperture of radius 3 arcseconds, we define the quantity $\delta \equiv m_2 - m_3$. The exact value of this quantity for a point source will depend upon the size of the PSF. Since the SDF images in all passbands have the same size (a FWHM of $0\farcs98$ arcseconds), we expected that stars would have roughly the same value of δ in all passbands. Our inspection of the images and catalogs showed this to be true: in all images, isolated stars fell into the range $0.10 < \delta < 0.18$.

In order to create a "clean" set of stars, we combined the two types of morphological information in the following manner. We looked at the information for each object in the SDF catalogs, as measured in each of the five wide passbands: B, V, R_c, i', z'. Each object was given an initial score of zero. For every `class_star` value in a passband which fell into the acceptable range of $0.90 - 1.00$, we added 1 to its score. For every δ value in a passband which fell into the acceptable range $0.10 - 0.18$, we added 1 to its score. The maximum score for a truly point-like object was therefore 10: 5 acceptable values of `class_star` and 5 acceptable values of δ. The minimum score, for an object which was obviously extended in all five passbands, was 0.

The two methods yield similar results, as one would expect: 8570 objects out of the 209,452 in the SDF catalogs have a `class_star` value within the acceptable range in all five passbands, and 5431 objects of the 209,452 have a δ value within the acceptable range in all five passbands. A total of 3725 objects, or about 1.8% of all detected objects, score a perfect 10, showing star-like shapes in all five passbands.

However, not all of these objects really are stars. We know from many previous studies (e.g. Johnson & Morgan 1953 , Newberg & Yanny 1997 , Finlator et al. 2000) that stars inhabit a rather narrow and well-defined region in color-color space. We choose three colors based on the wide-band `isocor` magnitudes reported in the SDF catalogs: $(B - V)$, $(V - R_c)$, $(R_c - z')$. If we plot the locations of the star-like objects in the space defined by these colors (see Figure 1), we see two main groups of objects: a set of mostly bright sources which form a relatively narrow band, and a set of mostly faint sources which spread out over a larger region. Because the brighter sources fall into the region of color space populated by stars in other studies, and because galaxies are expected to outnumber stars greatly at fainter magnitudes, we focus on the brighter sources to define our stellar locus. We created a "clean" sample of objects believed to be stars by choosing objects between $20.5 < R_c < 22.0$ with morphological scores 10 out of 10, and discarding the few outliers which fell far from the main group. Our final sample contains 351 objects.

As a check that our "clean" sample really does consist of stars, we examined the proper motions of objects of objects with morphological scores of 10 out of 10. The USNO B1.0 catalog

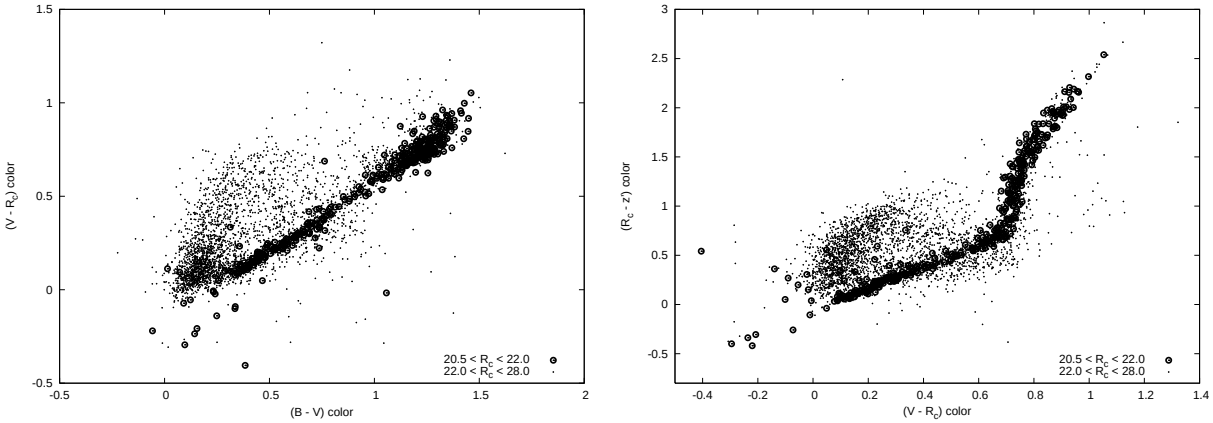

Fig. 1. Colors of objects with morphological score of 10 out of 10: very point-like shapes.

(Monet et al. 2003) provides proper motions for a small fraction of the brightest objects in the SDF. We determined that spurious matches between the catalogs outnumber true matches when the matching radius is about 1.0 arcsecond; within this radius, only about 20 percent of the matches are spurious. We therefore matched items in the USNO B1.0 catalog to objects with morphological scores of 10 out of 10, using a tolerance of 1.0 arcsecond. Table 1 shows the properties of the relatively small number of objects matched to USNO B1.0 entries. The majority of matched items have proper motions listed as zero; however, for those with non-zero values, objects within our "clean" subset clearly have larger motions than those we discarded. Moreover, the measured proper motions are largest for the red half of our "clean" subset, as one would expect if the cool stars were dwarfs. We conclude that the proper motions provide a weak piece of evidence that our "clean" sample is dominated by real stars, though we cannot be sure without spectra for each candidate.

Within our three-dimensional color space, stars inhabit a region which twists and turns. In order to follow this locus accurately, we follow the instructions given by Newberg & Yanny 1997 (see also Richards et al. 2002) to build a three-dimensional volume which contains the stars. These authors note that the stellar locus can be well approximated by a tube which is elliptical in cross section and changes shape and orientation as it moves from hot, blue stars to cool, red ones. The basic idea is to build the stellar locus iteratively: start by placing a few "locus nodes" in the middle of the stellar distribution (we started with three), then insert new locus nodes between existing ones. The stars surrounding each locus node are used to define an ellipsoidal tube which runs between it and its neighbors. Our code follows the algorithm described by Newberg & Yanny 1997 very closely; we added only one feature, a condition on the minimum number of stars which must belong to a locus node in order for it to be allowed to split (we needed this condition because the number of stars in our dataset was much smaller than those in most other situations).

After 100 iterations of the algorithm, our initial set of 3 locus nodes grew to 22 locus

nodes. The nature of this technique forces the nodes at each end of the locus to migrate inwards, leaving a sparse set of objects exposed at both the blue and red end. After examining the colors of all objects in the field surrounding the ends of the locus, and considering the synthetic colors of stars of very early and very late spectral types (see Section 3), we extended the locus at each end by adding one node manually. Since these nodes were not defined by a set of associated objects following the algorithm, they did not have a well-defined ellipsoidal tube. Therefore, we assigned to each of these extended nodes a circular tube with radius equal to the major axis of the nearest normal locus node.

In Table 2, we list the nodes which make up our stellar locus. We provide the location of each node in color-color space, the major (a) and minor (b) axes of the ellipse defined by star surrounding the node, and the angle (in radians) describing the orientation of the major axis of that ellipse (see Newberg & Yanny 1997 for details of the coordinate system used to define this angle). We also list a quantity we shall call the "milestone:" the distance along the stellar locus from locus number 1 to a location along the locus, measured by moving from locus node to locus node in straight line segments. The two end nodes, numbered 0 and 23, are the extensions we added manually. The columns for a and b show that, as others have found in different datasets, stars lie within a relatively narrow and flattened ribbon in color space: the ellipse describing the stellar locus has a width of less than 0.08 magnitudes, and a major axis usually two or more times larger than its minor axis.

3. Stellar Types along the Locus

The stellar locus we have created is simply a map of the region in color-color space in which stars are likely to fall. It does not provide any information on the nature of stars as a function of their position along this locus. However, if we can calculate the location in this same color space of either real stars with known properties, or models of stellar atmospheres, then we can draw a connection between the colors of any star in the SDF and its physical nature: spectral type, temperature, and even, to a lesser degree, luminosity or mass.

Therefore, we computed synthetic colors for several sets of stars with good spectrophotometry and known spectral class. We adopted the overall response curves for Suprime-Cam shown in Figure 1 of Kashikawa et al. 2004; that is, the curves which include the effects of both instruments and atmosphere. We then convolved two sets of spectra with these passbands to generate synthetic photometry:

- Pickles 1998 , each entry of which is the composite of several observed spectra
- Gunn & Stryker 1983 , each entry of which is the observed spectrum of a single star

Since the zeropoint of the magnitude scales are not simply related to the stars found in the Gunn & Stryker 1983 library, and since the Pickles 1998 data have been normalized to an arbitrary scale, we shifted the zeropoints of our synthetic magnitudes by a small amount so

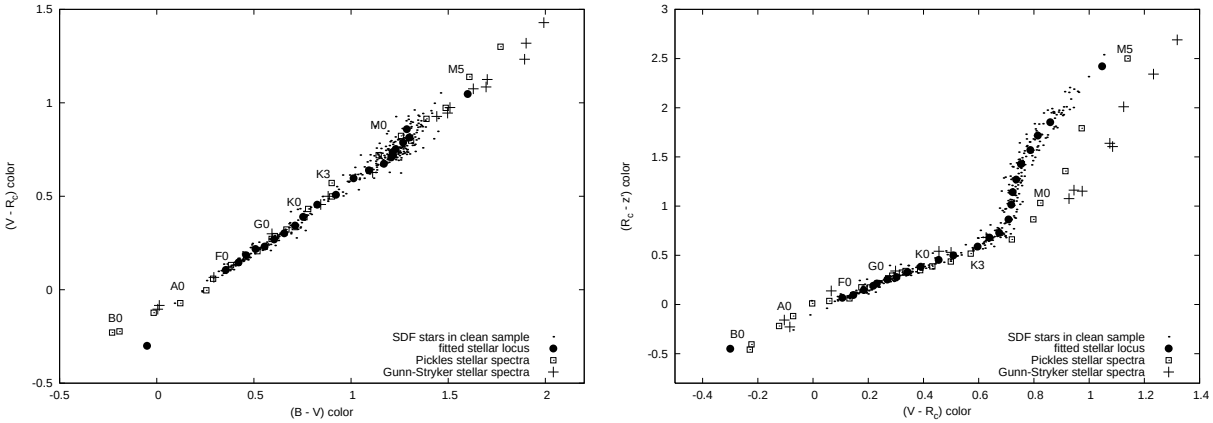

Fig. 2. Observed colors of stars in the SDF compared to synthetic colors of main-sequence stars in spectrophotometric atlases. The labels correspond to colors of stars from Pickles 1998 .

that the synthetic colors best matched the observed colors. We compare the observed colors to the synthetic colors of main sequence stars in Figure 2, placing labels for each spectral class based on main sequence stars from Pickles 1998 . The synthetic colors lie in the same locations as the observed colors for the most part, but there are a few regions in which they differ.

At the blue end of the stellar locus, there are very few observed stars: the bluest node defined by stars in our "clean" sample corresponds roughly to spectral class A7. In order to extend the locus to hotter stars, we relied in part on the synthetic colors, but also gave some weight to the observed positions of very blue, nearly point-like objects in the SDF catalogs. Especially in the graph of $(V - R_c)$ vs. $(B - V)$, our extended locus strays somewhat from the synthetic colors. It would be best, of course, to use observations of a field containing very blue stars to define this end of the locus.

At the cool end of the locus, we again find very few stars in the "clean" sample in the SDF. This is largely a selection effect, as explained in Section 5 below. The last node created by our automatic algorithm corresponds roughly to spectral type M3; we added one more node to the locus guided by the colors of the very few reddest stars measured in the SDF.

The obvious discrepancy between the observed colors and synthetic colors of cool stars (spectral classes K5 - M5) is due to differences in metallicity. The cool main-sequence Pickles and Gunn-Stryker stars were chosen to be bright enough ($9 < V < 13$) to yield spectra with high signal. Since these cool dwarfs have low luminosities, they must be within roughly 20 pc of the Sun, and thus members of the disk population with high metallicity. Any M dwarfs observed in the SDF, on the other hand, appear roughly ten magnitudes fainter than the spectrophotometric standards. They are therefore roughly 100 times more distant, at distances of several kpc from the Sun and the disk. We expect them to have lower metallicities. As a check, we convolved model stellar spectra of Lejeune et al. 1997 and Lejeune et al. 1998 with the Suprime-Cam passbands and computed their colors. We found that as the metallicity of cool main-sequence

dwarfs decreases from $[Fe/H] = 0.0$ to $[Fe/H] = -2.0$, the bend in the stellar locus in the $(R_c - z')$ vs. $(V - R_c)$ diagram becomes sharper, matching the observed stellar locus.

Despite this shift at the cool end, we believe that the progression of spectral types along the observed locus will mirror the progression of spectral types in the spectral libraries. Therefore, we assign a spectral class to objects along the observed stellar locus in the following manner: for each main spectral class (A0, B0, etc.), we compute synthetic colors based on the Pickles 1998 spectrophotometry. We then find the location along the observed stellar locus which is closest in three-dimensional color space to the theoretical value, and note the "milestone" (distance along the locus measured from node 1) at that location. Table 3 lists the relationship between spectral class and a measured property of objects in the SDF. Once we have found the position of an observed star in the SDF along the stellar locus, we can use its "milestone" to estimate a rough spectral class.

We remind the reader that the bright, point-like objects in the SDF which we use to construct the stellar locus span a somewhat limited range of spectral types: from about A7 at the blue end to about M3 at the red end. Using our locus to assign spectral class to stars outside this range is less reliable.

4. Using the Stellar Locus to Identify Stars

In Section 2, we used a small set of relatively bright, point-like objects – the "clean" sample of 351 stars – to build a stellar locus in color space. We can now apply this locus as a tool to search for additional stars in the total set of objects in the SDF catalogs. We describe in this section a method which gives each object a "color-based" probability of being a star, which is independent of the "shape-based" probability described earlier. A combination of both methods yields a more reliable sample of stars than either method alone.

The procedure for computing the "color score" of an object begins with its location in the three-dimensional color space of $(B - V)$, $(V - R_c)$, $(R_c - z')$. We find the position along the stellar locus which is closest to the star's color. We then ask the question: is the distance of this star from the stellar locus inside or outside the ellipsoidal tube defined by stars surrounding the locus at this location? The Newberg & Yanny 1997 algorithm determines the elliptical shape of the tube at each locus node, defined in a plane which is perpendicular to the line segment joining one locus node to the next. Following their example, we extend the ellipse outwards to its 3σ boundary; in other words, we make the extent of the tube large enough that it contains (on average) 98% of the stars in the local region of color space. Now, in general, a stellar candidate will be closest to some location between two locus nodes: call them P_i and P_{i+1}. In some sections of the stellar locus, such as the stretch from spectral class F0 to spectral class G0, the locus lies along a straight line in color space, and the elliptical shape remains relatively constant. But in other regions, such as the stretch from spectral class K0 to spectral class M0, the locus makes sharp bends and twists. If the shape and orientation of the tube at

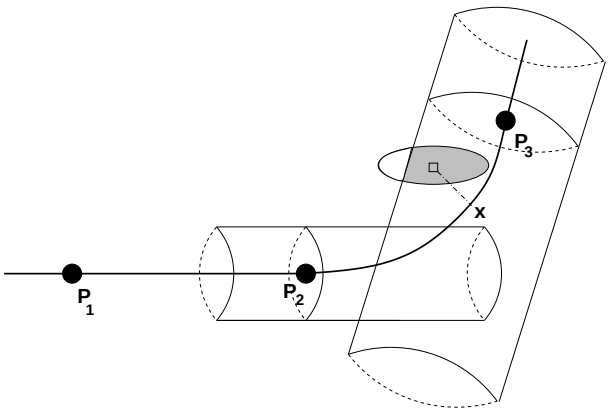

Fig. 3. Giving an object its "color score:" the observed colors of an object (square) place its closest approach to the stellar locus, at x, between locus nodes P_2 and P_3. The cloud of test positions around the object lies partially within the tube extending backwards from P_3. This object will receive a "color score" of about 0.75.

P_i are somewhat different than the shape and orientation at P_{i+1}, which elliptical parameters should we use when evaluating the nature of a candidate between them?

We take an inclusive approach: we extend the tube forward from locus node P_i using its parameters and determine whether the candidate lies inside or outside that tube; and we also extend the tube backwards from locus node P_{i+1} using *its* parameters and determine whether the candidate lies inside or outside that tube. If the candidate lies within either tube, then we consider it consistent with the stellar locus. A candidate must lie outside both tubes to fail the test. The candidate shown by a square in Figure 3 falls outside the tube extended forward from locus node P_2, but inside the tube extended backwards from P_3.

There is an additional complication: the magnitudes for every object in the SDF catalogs contain a tabulated uncertainty, which means that the colors derived from those magnitudes also have associated uncertainty. We use a Monte Carlo approach to assign a score to each object in the following way: for each real observed object, we generate $N = 100$ test points by adding random gaussian errors to the measured magnitudes B, V, R_c, z'. These test points appear as a cloud in color space surrounding the actual measured position of an object. Following the method described above, we determine if each of these test points lies inside or outside the stellar locus. We then assign a "color score" to the object which is simply the fraction of all test points which fall within the stellar locus. For example, roughly three-quarters of the test points around the object in Figure 3 fall within the tube extending backwards from locus node P_3; therefore, this object would receive a "color score" of about 0.75.

We have applied this procedure to all the objects in the SDF R_c-based catalog, regardless of their shape or size. A summary of the results is shown in Table 4. It is clear that color provides a sharper tool than shape to divide stars from galaxies. For example, roughly 12% of all sources have shapes in the different images which are at least somewhat point-like (scoring

at least 5 out of 10 on the morphological scale), but fewer than 2% of all sources have colors which are somewhat star-like (scoring at least 0.5 out of 1.0 on the color scale).

5. Discussion

Before we can interpret the results of our classification, we need to account for the selection effects in its construction. The original SDF observations had a range of total exposure times, from 340 minutes in V-band to 801 minutes in i'-band. The resulting images reach different depths. We have concentrated on the catalogs produced based on detections in the R_c images, and requiring matching detections in the other passbands. If we examine the distribution of objects as a function of magnitude in each passband, we find a similar pattern in each case: a few very bright objects, then increasing numbers of fainter objects, reaching a peak at some particular magnitude and then declining. The peak of this distribution is fainter for fuzzy sources than for point-like sources in B, V, R_c, but roughly the same for z'. It is important that the peak magnitude is not the same in all passbands: we find the peak for point-like objects to be between 25.4 and 25.8 for B, V and R_c, but only 24.4 for z'; we will refer to these values as the "multicolor completeness limit" for point sources.

This creates a significant bias against faint objects of extreme colors in the catalogs. Very blue objects (say, stars of spectral type B8) which are close to the plate limit in the R_c band will fail to appear in the z' images and so not be included in the catalogs. Very red objects (say, stars of spectral type M3), on the other hand, which are barely detected in the z' images will not appear at all in the B or V images, and so again fall out of the catalogs. In order to compare our results to those in other regions of the sky, we need to include the effects of these selection biases.

We have found the galactic population model produced by astronomers at the Besançon Observatory (Bienaymé, Robin, & Crézé 1987 , Haywood, Robin and Crézé 1997 , Robin et al. 2003 ; hereafter "the Besançon model") very useful, especially since it is easy to run interactively: see `www.obs-besancon.fr/modele/modele.html`. We generated a simulation of stars that should appear within the region of the SDF, using the default Besançon model parameters and a maximum V-band observed magnitude of 28.0. If we compare the simulation to the objects classified as stars by our algorithm (see Figure 4), we see that our catalog follows the model only until magnitude $V \sim 23$. However, if we generate magnitudes in the SDF passbands for each star in the model, and discard any star which falls below the multicolor completeness limit for point sources in our input catalogs ($B = 25.8$, $V = 25.6$, $R_c = 25.4$, $z' = 24.4$), then we find the number of stars in the model matches the number of objects we classify as stars reasonably well.

The good agreement between our sample of objects classified as stars and the Besançon model suggests that we may use the model to provide insight into some properties of our sample. For example, we note that of the 1786 stars in the Besançon model which would qualify as stars

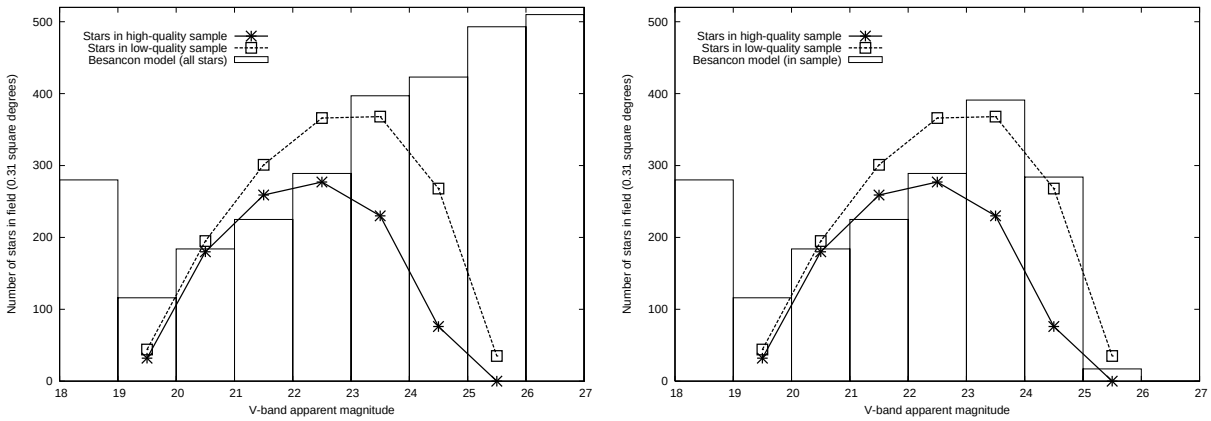

Fig. 4. Counts of objects classified as stars by our algorithm and stars in the Besançon model of the field, as a function of V-band magnitude. In the right-hand panel, we have discarded stars from the model which would not appear in the input to our algorithm.

in our algorithm, only 36, or roughly 2%, have evolved far off the main sequence. If the great majority of stars we observe are on the main sequence, then we would not expect to see any significant split of the stellar locus into two tracks for giants and dwarfs. As described above in Section 3, we indeed do not see any indication of a bifurcation in the stellar locus. Moreover, we are apparently justified in using spectra of main sequence stars to compute synthetic colors in the Suprime-Cam system. The Besançon model also predicts that many of the cool stars in our observed sample ought to have low metallicities, which again agrees with the observations.

As an additional check on our separation of stars from galaxies, we considered proper motions. Using a 1-arcsecond radius, we found 1605 matches between the SDF catalog and the USNO B1.0; 253 of these matched objects fell into our "low-quality star" category, while the remaining 1352 were classified as non-stellar. A majority (58%) of objects classified as stellar had a non-zero proper motion, while a smaller fraction (37%) of the objects classified as non-stellar had a non-zero proper motion. At the current time, this kinematic evidence only weakly supports our claim to identify stars. We hope to revisit the issue after future observations provide more precise measurements of proper motions.

Our algorithm not only separates stars from galaxies based on their colors, but also provides rough spectral classifications, as shown in Table 3. We show the distribution of "milestone" values for the objects classified as stars in Figure 5. Both the high-quality and low-quality samples show a similar pattern: the distribution of the brightest stars is somewhat bimodal, the majority located at either the blue end (spectral type A-F) or red end (spectral type M) of the stellar locus. Other photometric studies of our galaxy at these magnitudes (Infante 1986 , Infante 1994 , Prandoni et al. 1999) show this double-peaked distribution. The standard explanation (e.g., Bahcall 1986) is that the blue peak indicates the main-sequence turnoff point of metal-poor halo stars, while the red peak is due to the competition between

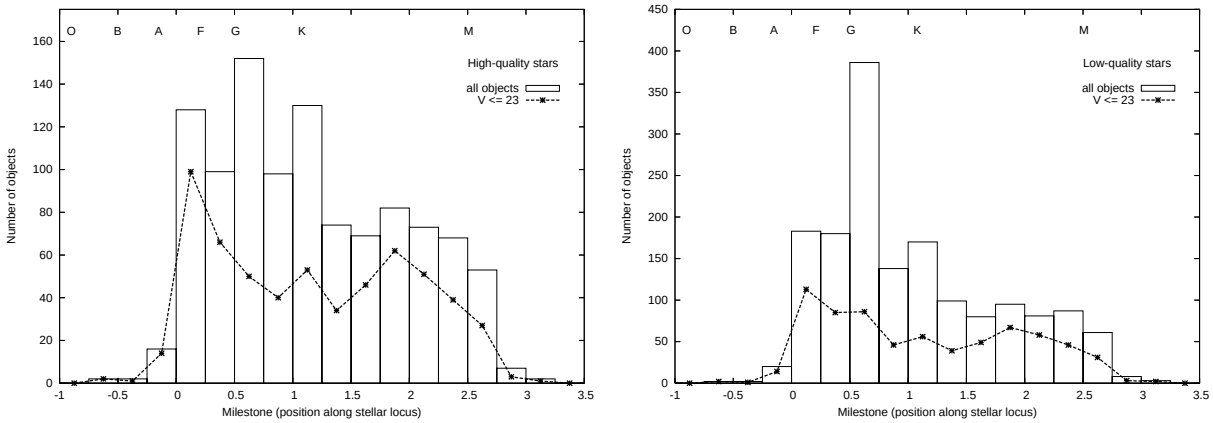

Fig. 5. Distribution of the "milestone" values (location along the stellar locus) of objects classified as stars. The labels at top are in the middle of each spectral type's range.

increasing number and decreasing luminosity of low-mass disk stars.

In both samples, however, when we look fainter than the multicolor completeness limit, we see a large number of objects with intermediate colors. The excess is especially obvious in the low-quality sample. We examined these faint, intermediate-color objects carefully to see if there might be some obvious explanation. They do not show any clumping or patterns in their (RA, Dec) positions in the field, so they are not artifacts of diffraction spikes or halos around bright objects. A significant fraction, perhaps one-third, of the items which appear only in the low-quality sample are blends of two or more objects; it makes some sense that blended objects would have typical colors in between those of individual objects. Some of these sources appear slightly elliptical, and may be nearly round galaxies. However, we also find that many of these objects appear to be reasonably isolated and point-like. Could there really be an increase in the number of stars of intermediate color at magnitudes $V > 23$? We remind the reader that this is below our multicolor completeness limit, so that many stars at both the blue and red ends of the population are not included in the sample. We also note that a main-sequence G star of absolute magnitude $M_V \sim 5$ and apparent magnitude $m_V \sim 24$ would be located at a distance of roughly $d \sim 60$ kpc, very far from both the plane and the bulge of the Milky Way Galaxy. The Besançon model does not show this feature. If this feature is real, we speculate that it might be due to a local perturbation to the normal halo population, perhaps the remnant of some disrupted satellite galaxy or globular cluster. According to Martínez-Delgado et al. 2001 and Majewski et al. 2003 , the SDF lies within ten degrees of the northarm arm of the Sagittarius Dwarf stream, which has a distance of roughly 50 kpc from the Sun at this location.

6. Conclusions

We have used one set of the Subaru SDF catalogs, based on detections in the R_c images and corresponding measurements in in B, V, R_c and z', to study stars in the SDF. We used both

Table 1. Proper motion (PM), in units mas/yr, of objects with morphological scores 10 out of 10

Subset	Number	$PM > 0$	For objects with $PM > 0$		
			mean	stdev	median
in clean set, $(V - R_c) < 0.6$	64	20%	57	68	37
in clean set, $(V - R_c) > 0.6$	58	31%	74	60	43
outside clean set	36	22%	12	4	12

morphological and color information to choose a small set of certain stars, around which we created a stellar locus in three-dimensional color space. We then compared the location in color-space of *all* sources in the SDF catalogs to the stellar locus. The results provide a quantitative measure which not only distinguishes stars from galaxies, but also assigns rough spectral types to the stellar candidates. We find good agreement between the Bescançon model of the Milky Way and number counts of stars in the SDF down to our "multicolor completeness limit" (which is several magnitudes brighter than the detection limit in any individual passband). Our catalog of objects in the SDF, which includes their proximity to and position along the stellar locus, can be found at `http://spiff.rit.edu/sdf/`.

We thank the referee, Heidi Newberg, for suggestions which improved the paper.

References

Bahcall, J. N. 1986, A&RAA, 24, 577
Bertin, E, & Arnouts, S. 1996, A&AS, 117, 393
Bienaymé, O., Robin, A. C., & Crézé, M. 1987, A&A, 180, 94
Finlator, K. et al. 2000, AJ, 120, 2615
Gunn, J. E. & Stryker, L. L. 2000, ApJS, 52, 121
Haywood, M., Robin, A. C., & Crézé, M. 1997, A&A, 320, 440
Infante, L. 1986, PASP, 98, 360
Infante, L. 1994, A&AS, 107, 413
Johnson, H. L. & Morgan, W. W. 1953, ApJ, 117, 313
Kashikawa, N. et al. 2004, PASJ, 56, 1011
Lejeune, T., Cuisinier, F. & Buser, R. 1997, A&AS, 125, 229
Lejeune, T., Cuisinier, F. & Buser, R. 1997, A&AS, 130, 65
Majewski, S. R. et al. 2003, ApJ, 599, 1082
Martínez-Delgado, D. et al. 2001, ApJ, 549, L199
Monet, D. G. et al. 2003, AJ, 125, 984
Newberg, H. J. & Yanny, B. 1997, ApJS, 113, 89
Pickles, A. J. 1998, PASP, 110, 863
Prandoni, I. et al. 1999, A&A, 345, 448
Richards, G. T. et al. 2002, AJ, 123, 2945

Table 2. The stellar locus.

Node	$(B-V)$	$(V-R_c)$	(R_c-z')	Milestone	a	b	θ
0	-0.050	-0.300	-0.450	-0.773	0.0258	0.0258	2.85
1	0.355	0.106	0.068	0.000	0.0258	0.0122	2.85
2	0.421	0.146	0.096	0.082	0.0145	0.0077	2.79
3	0.460	0.184	0.147	0.156	0.0375	0.0163	3.02
4	0.508	0.218	0.190	0.229	0.0310	0.0156	2.90
5	0.555	0.231	0.213	0.283	0.0282	0.0120	2.65
6	0.604	0.269	0.253	0.356	0.0204	0.0132	2.92
7	0.656	0.302	0.279	0.424	0.0220	0.0122	3.09
8	0.712	0.343	0.329	0.509	0.0356	0.0239	0.18
9	0.753	0.390	0.384	0.592	0.0342	0.0263	1.32
10	0.826	0.455	0.453	0.712	0.0463	0.0116	3.02
11	0.922	0.508	0.499	0.831	0.0327	0.0148	2.89
12	1.013	0.596	0.589	0.986	0.0390	0.0217	2.62
13	1.092	0.639	0.680	1.114	0.0431	0.0208	2.92
14	1.169	0.674	0.729	1.212	0.0529	0.0259	2.81
15	1.207	0.708	0.864	1.356	0.0573	0.0134	2.50
16	1.215	0.718	1.015	1.507	0.0570	0.0167	2.35
17	1.215	0.723	1.142	1.634	0.0394	0.0163	1.73
18	1.214	0.736	1.270	1.763	0.0546	0.0180	2.25
19	1.230	0.753	1.427	1.922	0.0575	0.0185	2.49
20	1.268	0.787	1.570	2.074	0.0566	0.0176	2.68
21	1.299	0.814	1.717	2.227	0.0673	0.0215	1.99
22	1.287	0.859	1.853	2.388	0.0717	0.0291	1.51
23	1.600	1.047	2.421	3.063	0.0717	0.0717	1.51

Robin, A. C., Reylé, C., Derrière, S., & Picaud, S. 2003, A&A, 409, 523
Williams, R. E. et al. 1996, AJ, 112, 1335

Table 3. Conversion from position along stellar locus to spectral class.

Start milestone	End milestone	Spectral class
-1.00	-0.77	O
-0.77	-0.34	B
-0.34	0.03	A
0.03	0.38	F
0.38	0.63	G
0.63	1.53	K
1.53	3.50	M

Table 4. Summary of classification of 189,380 sources in SDF R_c-band catalog.

Shape score (0 - 10)	Color score (0.0 - 1.0)	Number of objects	Category name
$0-1$	$0.0-1.0$	127,359	non-stellar shape
$0-10$	$0.0-0.1$	185,819	non-stellar colors
$5-10$	$0.0-1.0$	22,157	somewhat stellar shape
$9-10$	$0.0-1.0$	6348	very stellar shape
$0-10$	$0.5-1.0$	2711	somewhat stellar colors
$0-10$	$0.9-1.0$	2024	very stellar colors
$5-10$	$0.5-1.0$	1595	low-quality stars
$9-10$	$0.9-1.0$	1061	high-quality stars